

Supplementary information

A single-interface photoelectrochemical sensor based on branched TiO₂ nanorods@strontium titanate for two biomarkers detection

Jie Xue,^a Chaomin Gao,^a Lina Zhang,^{*b} Kang Cui,^{*a} Wenxing He,^c and Jinghua Yu^a

^a*School of Chemistry and Chemical Engineering, University of Jinan, Jinan 250022, P.R. China.*

^b*Shandong Provincial Key Laboratory of Preparation and Measurement of Building Materials, University of Jinan, Jinan 250022, PR China.*

^c*School of Biological Sciences and Technology, University of Jinan, Jinan 250022, China.*

*Corresponding author: Lina Zhang and Kang Cui

E-mail: mse_zhangln@ujn.edu.cn

E-mail: chm_cuik@ujn.edu.cn

S1. Experimental

S1.1 Materials and reagents

Fluorine-doped tin oxide (FTO) glass substrate with a thickness of 2.2 mm (resistance of $< 15 \Omega/\text{sq}$) was purchased from Xiamen FTO Photoelectricity Industry (Xiamen, China). The cancer antigen 153 (CA 153), alpha fetoprotein (AFP), the primary capture antibody and secondary detection antibody of them were purchased from China Shanghai Linc-Bio Science Co. Ltd. Ultrapure water obtained from a Millipore water purification system ($\geq 18 \text{ M}\Omega \text{ cm}$, Milli-Q, Millipore) was used in all assays and solutions. Glutaraldehyde (GA), Chitosan (CS) and bovine serum albumin (BSA) were purchased from Alfa Aesar China Ltd. The acetylthiocholine chloride (ATC), p-aminophenyl galactopyranoside (PAPG), streptavidin, β -galactosidase (β -Gal), and acetylcholinesterase (AChE) were purchased from Sigma-Aldrich (Shanghai, China), in which the β -Gal and AChE were labeled with streptavidin by Beijing Biosynthesis Biotechnology Co., LTD. Other chemicals were analytical reagent grade and used as received. The blocking buffer was 0.01 M PBS (pH 7.4) containing 3% (w/v) BSA. 0.01 M PBS (pH 7.4) was used for the preparation of the antigen and antibody solutions. The washing buffer solution was 0.01 M PBS (pH 7.4) containing 0.05 % Tween 20. All chemicals were of analytical grade and were used as received.

S1.2 Apparatus

PEC measurements were performed using a homemade PEC system. A 500 W xenon arc lamp (CHF-XQ-500 W, Beijing Changtuo Co., Ltd.) equipped with a monochromator was used as the irradiation source. Electrochemical impedance spectrum (EIS) was carried out on an IM6x electrochemical station (Zahner, Germany). Scanning electron microscopy (SEM) images were recorded using a QUANTA FEG 250 thermal field emission scanning electron microscopy (FEI

Co., USA), The phase characterization was performed by X-ray diffraction (XRD) using a D8 advance diffractometer system equipped with Cu K α radiation (Bruker Co., Germany). Photocurrent was measured by the current–time curve experimental technique on a CHI660D electrochemistry workstation (Shanghai CH Instruments Co., China) with a three-electrode system. PL analysis was carried using Fluorolog-3 Spectrofluorometer (Horiba Scientific, New Jersey, USA) equipped with a Nd:YAG laser system with an excitation wavelength at 325 nm. X-ray photoelectron spectroscopy (XPS) was performed on a VG ESCALAB LKII instrument with Mg KR ADES ($h\nu = 1253.6$ eV) source at a room temperature at a base pressure of below 10^{-8} Pa.

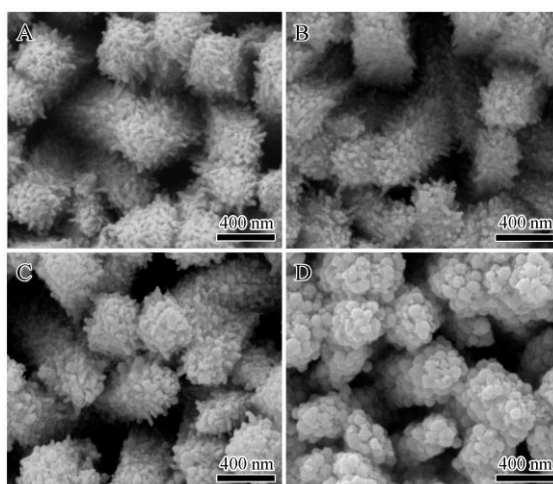


Fig. S1 The SEM images of the (A) B-TiO₂ NRs, B-TiO₂ NRs@SrTiO₃ obtained after (B) 30 min, (C) 45 min and (D) 1 h hydrothermal conversion at 160 °C.

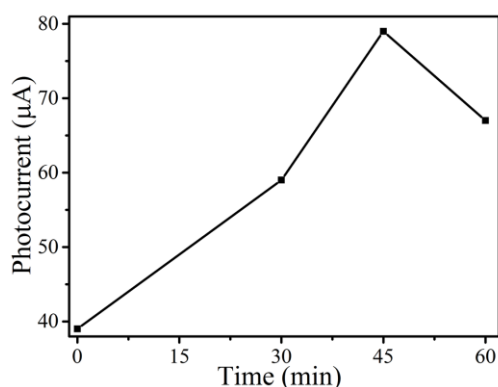


Fig.S2 Photocurrent response vs the different reaction time of B-TiO₂ NRs in strontium hydroxide solution at 160 °C.

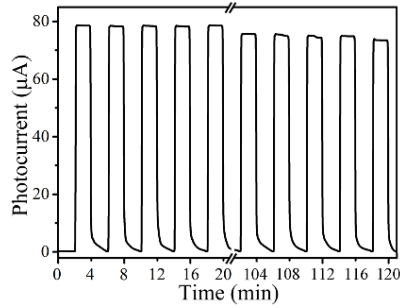


Fig.S3. The photo-stability of the B-TiO₂ NRs@SrTiO₃ heterojunction.

To study the photo-stability of the B-TiO₂ NRs@SrTiO₃ heterojunction, 30 continue on/off cycles were performed with the B-TiO₂ NRs@SrTiO₃ electrode. For each cycle, the on and off time were both 2 min. As can be seen from Fig. S3, the photocurrent of the photoelectrode did not show obvious decrease, indicating good photo-stability of the B-TiO₂ NRs@SrTiO₃ heterojunction.

S2. Optimization of detection conditions

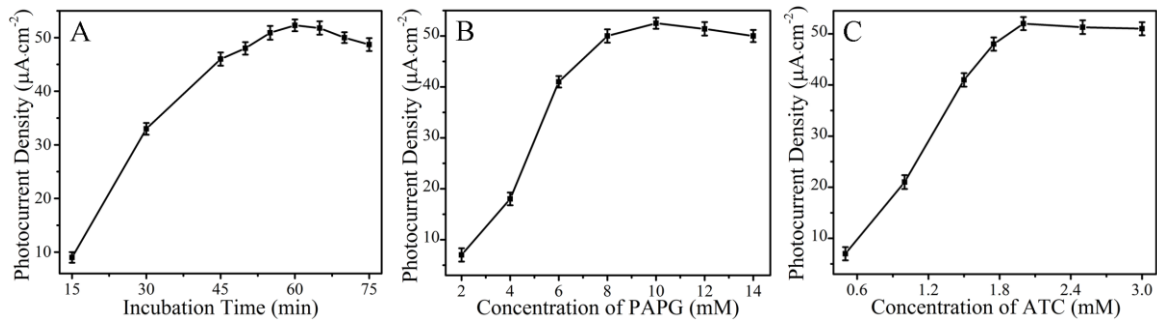


Fig. S4 (A) The effect of incubation time of the mixed antigen on photocurrent intensity. (B) The effect of PAPG concentration on photocurrent intensity. (C) Effect of ATC concentration on photocurrent intensity.

In order to obtain the best performance, some factors that influence the signal response of the sensor were optimized. Fig. S4A shows the relationship between incubation time of mixed antigen and the photocurrent intensity. As can be seen, with the increase of the incubation time, the photocurrent intensity gradually increased and reached a plateau after 60 min, indicating that the 60 min is enough to complete the response. Therefore, 60 min was selected as the optimal incubation time and used in this study. Fig. S4B shows the relationship between the concentration of PAPG and the photocurrent intensity. The photocurrent intensity increases rapidly with the

increase of PAPG concentration before 10 mM. When the PAPG concentration exceeds 10 mM, the photocurrent intensity was not significantly increased. Therefore, 10 mM was selected as the optimal PAPG concentration. Similarly, Fig. S4C shows the effect of ATC concentration on the photocurrent intensity. As seen, when the concentration of ATC does not exceed 2 mM, the photocurrent intensity increased with the increasing of the ATC concentration. However, when the concentration of ATC was greater than 2 mM, the photocurrent intensity does not change obviously. Thus, 2 mM was chosen as the optimum of the ATC concentration.

S3. Analytical electrode interference

Table S1. The interaction between the β -Gal and AChE. The numbers in the table represent the photocurrent increments before and after enzyme catalysis in the corresponding solution.

| Substrate solution | β -Gal | AChE | Enzyme mixture |
|--------------------|--------------|--------|----------------|
| PAPG-PBS | 7.085 | -1.358 | 6.085 |
| ATC-PBS | -1.174 | 5.749 | 4.928 |

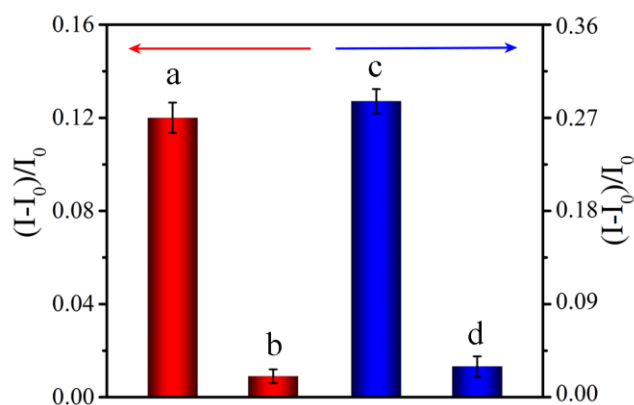


Fig. S5. Photocurrent increment of (a) mixed antigens and (b) mono AFP after incubation in PAPG-PBS solution; Photocurrent increment of (c) mixed antigens and (d) mono CA 153 after incubation in ATC-PBS solution. The used antigens are 10 ng mL⁻¹ AFP and 1 ng mL⁻¹ CA 153. I₀ was the photocurrent in PBS solution, and I was the photocurrent after incubation in the corresponding substrate solution.

Table S2A. The comparison for different AFP detection methods.

| Method | Detection range | Detection limit | References |
|-------------------------|-------------------------------|--------------------------|------------|
| Electrochemical | 0.025-15 ng mL ⁻¹ | 12 pg mL ⁻¹ | 1 |
| Chemiluminescent | 0.05-50 ng mL ⁻¹ | 40 pg mL ⁻¹ | 2 |
| Electrochemiluminescent | 0.001-200 ng mL ⁻¹ | 32 pg mL ⁻¹ | 3 |
| Fluorescent | 0.05-20 ng mL ⁻¹ | 17.3 pg mL ⁻¹ | 4 |
| PEC | 0.007-500 ng mL ⁻¹ | 1 pg mL ⁻¹ | This work |

Table S2B. The comparison for different CA 153 detection methods.

| Method | Detection range | Detection limit | References |
|-------------------------|-------------------------------|-------------------------|------------|
| Electrochemical | 0.05-100 ng mL ⁻¹ | 50 pg mL ⁻¹ | 5 |
| Chemiluminescent | 0.025-900 ng mL ⁻¹ | 3.4 pg mL ⁻¹ | 6 |
| Electrochemiluminescent | 0.005-500 ng mL ⁻¹ | 14 pg mL ⁻¹ | 7 |
| Fluorescent | 0.01-200 ng mL ⁻¹ | 9 pg mL ⁻¹ | 8 |
| PEC | 0.001-100 ng mL ⁻¹ | 0.2 pg mL ⁻¹ | This work |

S4. Applicability for clinical diagnosis

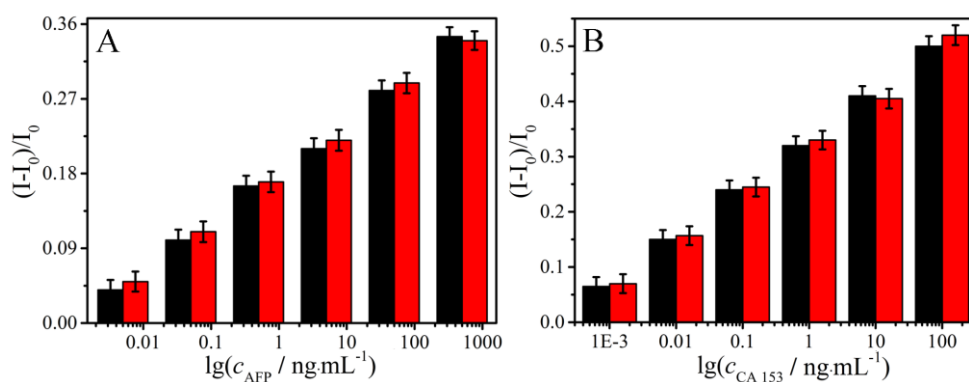


Fig. S6. Photocurrent increment of different (A) AFP concentrations and (B) CA 153 concentrations in PBS solution (black) and in 10% normal human serum (red).

References

1. J. Li, T. Gao, S. Gu, J. Zhi, J. Yang and G. Li, *Biosensors and Bioelectronics*, 2017, **87**, 352-357.
2. H. Gao, X. Wang, M. Li, H. Qi, Q. Gao and C. Zhang, *Biosensors and Bioelectronics*, 2017, **98**, 62-67.

3. Z.-J. Huang, W.-D. Han, Y.-H. Wu, X.-G. Hu, Y.-N. Yuan, W. Chen, H.-P. Peng, A.-L. Liu and X.-H. Lin, *Journal of Electroanalytical Chemistry*, 2017, **785**, 8-13.
4. Z. Lin, M. Li, S. Lv, K. Zhang, M. Lu and D. Tang, *Journal of Materials Chemistry B*, 2017, **5**, 8506-8513.
5. Y. Wu, P. Xue, K. M. Hui and Y. Kang, *Biosensors and Bioelectronics*, 2014, **52**, 180-187.
6. P. Li, H. Ye, J. Liu, H. Jin, Y. Lin, S. Yan, Y. Yu, L. Gao, F. Xu and Z. Zhang, *Journal of Clinical Laboratory Analysis*, 2018, **32**, 22158.
7. F. Liu, S. Ge, M. Su, X. Song, M. Yan and J. Yu, *Biosensors and Bioelectronics*, 2015, **71**, 286-293.
8. B. Zhang, W. Ma, F. Li, W. Gao, Q. Zhao, W. Peng, J. Piao, X. Wu, H. Wang, X. Gong and J. Chang, *Nanoscale*, 2017, **9**, 18711-18722.